ACS APPLIED MATERIALS & INTERFACES

Research Article

www.acsami.org

Gold Nanocluster-Conjugated Amphiphilic Block Copolymer for Tumor-Targeted Drug Delivery

Tong Chen,[†,‡] Shuang Xu,[†] Tong Zhao,[†] Ling Zhu,[†] Dongfeng Wei,[§] Yuanyuan Li,[†] Haixia Zhang,*[,†] and Chunyan Zhao*[,§]

[†]State Key Laboratory of Applied Organic Chemistry, Chemistry Department, and [§]School of Pharmacy, Lanzhou University, Lanzhou 730000, China

[‡]School of Environment and Chemical Engineering, Nanchang Hangkong University, Nanchang, 330063, China

ABSTRACT: Two kinds of core−shell structured multifunctional nanocarriers of gold nanoclusters (Au NCs) as core and folate (FA)-conjugated amphiphilic hyperbranched block copolymer as shell based on poly(L-lactide) (PLA) inner arm and FA-conjugated sulfated polysaccharide (GPPS−FA) outer arm (Au NCs-PLA-GPPS-FA) were synthesized for targeted anticancer drug delivery. The structure and properties of Au NCs-PLA-GPPS-FA copolymers were characterized and determined by ^{1}H NMR spectrum, FT-IR spectra, dynamic light scattering (DLS), fluorescence spectroscopy, and transmission electron microscopic (TEM) analyses. The anticancer drug, camptothecin (CPT) was used as a hydrophobic model anticancer drug. In vitro, two kinds of the nanocarriers presented a relatively rapid release in the first stage (up to 1 h) followed by a sustained release period (up to 15 h), and then reached a plateau at pH 5.3, 7.4, and 9.6. The release results indicated that CPT release from two kinds of the nanocarriers at pH 9.6 was much greater than that at both pH 5.3 and 7.4. The cytotoxicity studies showed that the CPT-loaded nanocarriers provided high anticancer activity against Hela cells. Furthermore, nanocarriers gained specificity to target some cancer cells because of the enhanced cell uptake mediated by FA moiety. The fluorescent images studies showed that the nanocarriers could track at the cellular level for advance therapy. The results indicated that the Au NCs-PLA-GPPS-FA copolymers not only had great potential as tumor-targeted drug delivery carrier, but also had an assistant role in the treatment of cancer.

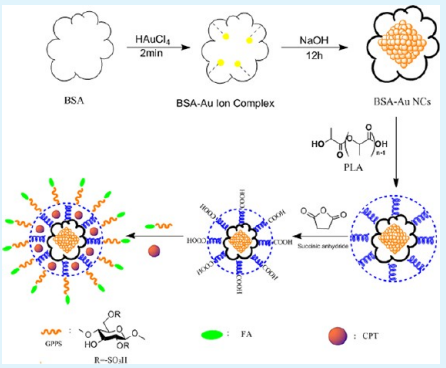

KEYWORDS: *nanocarriers, drug delivery, Au NCs, cytotoxicity*

INTRODUCTION

Metal nanoparticles (NPs) and nanoclusters (NCs) have attracted the attention of researchers because of their wide applications in the fields of chemistry, biology and materials.[1,2] There has been a great deal of research work on drug delivery of metal NPs and NCs, especially gold and silver.[3,4] For example, Au NPs with tetra(ethylene glycol)ylated cationic ligands and fluorogenic ligands were synthesized for hydrophobic drug delivery.[5] Prabaharan et al. recently synthesized Au NPs stabilized with a monolayer of folate-conjugated poly(L-aspartate-doxo-rubicin)-*b*-poly(ethylene glycol) copolymer as a tumor-targeted drug delivery carrier.[6]

Quantum-sized Au nanoparticles, also called Au nanoclusters (Au NCs), composed of very few atoms with a ultrasmall size ranging from subnanometer to approximately 2 nm (core diameter),[7] have drawn wide attention in recent years. Au NCs show a lot of important properties, such as enhanced catalytic activity, high fluorescence and unique charging properties,[8−11] which render the material promising in various areas, including catalysis, sensing, biological fluorescence labeling and medical research. Furthermore, Au NCs exhibit other fascinating features, including ease of synthesis, good water solubility, low toxicity, surface functionalities, biocompatibility, and excellent stability, which also make them hold great promise in biology and medicine.[12−14]

Bovine serum albumin (BSA)[15] is selected as the stabilizer and reducer to form fluorescent Au NCs in some studies. The reduction ability of BSA molecules is activated by adjusting the reaction pH to 12; the entrapped ions undergo progressive reduction to form Au NCs in situ. The as-prepared Au NCs consist of 25 gold atoms and are stabilized within BSA molecules as BSA-Au NCs bioconjugates. Besides the above advantages of Au NCs, the BSA coating layer on Au NCs also facilitate postsynthesis surface modifications with functional ligands due to the existence of the amine groups and the carboxyl groups.

Polysaccharides from plants are not only safe and biocompatible, but also biodegradable, which own many kinds of biological activities. Furthermore, molecular modification of polysaccharide were considered as a way to enhance the biological activities of polysaccharide. Recently, polysaccharide obtained from *Gynostemma pentaphyllum* Makino (GPP) has attracted great attention because of its antitumor

Received: July 4, 2012
Accepted: October 8, 2012
Published: October 8, 2012

activities, immunomodulatory effect and antioxidant properties.[16−18] In our previous work, the sulfated derivatives of GPP (GPPS) were synthesized by chlorosulfonic acid−pyridine method, and the GPPS had higher antitumor activities than the GPP.[19] On the basis of the above experimental results, GPPS could be used as a hydrophilic outer shell of drug carriers for better biocompatible and antitumor activities but low cytotoxicity to normal cells.

One of the greatest challenges facing chemotherapy today is developing drug delivery systems (DDSs) that are efficacious and have therapeutic selectivity.[20] Both passive and active targeting approaches have been utilized with nanocarriers such as dendrimers,[21] liposomes,[22] metal nanoparticles,[23] and polymer micelles. These DDSs have improved in the targeted delivery of the therapeutics for cancer treatment. Folate (FA) has become an attractive candidate molecule for targeting cancer cells because it is an essential vitamin for the biosynthesis of nucleotide bases and is consumed in elevated quantities by proliferating cells.[24,25] It is clear that FA conjugates are taken up nondestructively by mammalian cells via receptor-mediated endocytosis.

In this study, we synthesized core−shell structured multifunctional nanocarriers (Au NCs-PLA-GPPS-FA) of Au NCs as core and (FA)-conjugated amphiphilic hyperbranched block copolymer as shell based on poly(L-lactide) (PLA) inner arm and FA-conjugated GPPS (GPPS−FA) outer arm for targeted anticancer drug delivery. To the best of our knowledge, this was the first attempt to prepare drug carriers with certain antitumor activities due to GPPS as a hydrophilic outer shell. Au NCs could be used for fluorescence labeling. Amphiphilic hyperbranched block copolymer could improve nanocarriers stability and drug loading ability. FA-conjugated nanocarriers could be directed to the cancer cells and subsequently internalized in the target cell via receptor-mediated endocytosis. The structure and properties of nanocarriers were characterized and determined by ^{1}H NMR, FT-IR spectra, DLS, fluorescence spectroscopy and TEM analyses. Camptothecin (CPT) was used as a hydrophobic model anticancer drug. The drug loading and in vitro release behaviors were studied at different pH. In vitro cytotoxicity of Au NCs-PLA-GPPS-FA copolymers was investigated by employing Hela cells.

EXPERIMENTAL SECTION

Materials and Reagents. The crude GPP from *Gynostemma pentaphyllum* Makino (collected from the mountain area in Weinan City, Shaanxi Province, China) was obtained from Shaanxi Lixin Biotechnology Co. (China) and purified further in our laboratory. M_w of purified GPP was 9.3 kDa and its composition contained rhamnose and xylose, whose mol ratio was 1:12.25. The sulfated derivatives of GPP (GPPS) showed that the degree of substitution (DS) was 1.20, and M_w was 8.96 kDa.[19]

Sodium hydroxide (NaOH), triethylamine and FA were purchased from Tianjin Guangfu Chemical Research Institute (Tianjin, China). 1-(3-Dimethylaminopropyl)-3-ethylcarbodiimide hydrochloride (EDC.HCl), tetrachloroauric acid ($HAuCl_4$), N-hydroxy succinimide (NHS), and 4-dimethylamino pyridine (DMAP) were purchased from aladdin chemistry Co., Ltd. (Beijing, China). Succinic anhydride was obtained from Sinopharm Chemical Reagent Co., Ltd. (Beijing, China). PLA (M_w, 10000 and 15000) were purchased from Brightchina Co., Ltd. CPT was supplied by Lanbei Plant & Chemical Co., Ltd. (Chengdu, China). N,N-Dimethylformamide (DMF), dimethyl sulfoxide (DMSO) ethanol and dichloromethane (CH_2Cl_2) were analytical grade and obtained from Gansu Yinguang Chemical Industry Co. (China). 3-(4,5-Dimethylthiazol-2-yl)-2,5-diphenyltetrazolium bromide (MTT) and BSA was from Sigma Co. (France).

Synthesis of Red Fluorescent Au NCs. Au NCs were first obtained by the method described in the literature.[11] In a typical experiment, aqueous $HAuCl_4$ solution (5 mL, 10 mM, 37 °C) was added to BSA solution (5 mL, 50 mg/mL, 37 °C) under vigorous stirring. NaOH solution (0.5 mL, 1 M) was introduced 2 min later, and the reaction was allowed to proceed under vigorous stirring at 37 °C for 12 h. The product, Au NCs were dialyzed against deionized water using a dialysis tubing (molecular weight cutoff of 3 kDa) for 48 h and dried in vacuum.

Synthesis of Au NCs-PLA. Two grams of PLA (M_w, 10 000 and 15 000) was dissolved in 50 mL of anhydrous CH_2Cl_2, respectively. Then the surface carboxyl groups were activated by adding 50 mg of NHS and 80 mg of EDC·HCl and stirred at room temperature for 2 h. Au NCs (500 mg) were dissolved in 50 mL of anhydrous DMSO and added in the mixture. After 48 h, the reaction mixture was poured into cold diethyl ether, and a precipitate was collected by filtration and washed with diethyl ether, followed by drying in vacuum. The products were denoted as Au NCs-PLA-1 and Au NCs-PLA-2.

Synthesis of Au NCs−PLA with Carboxyl End Group (Au NCs−PLA−COOH). Au NCs−PLA−COOH was prepared by reacting 2 g of Au NCs−PLA with 100 mg of succinic anhydride in the presence of 120 mg of DMAP as a catalyst. The reaction was carried out in the mixture of triethylamine and anhydrous DMF (100 mL) for 24 h at room temperature under stirring. Thereafter, the product was dialyzed against deionized water using a dialysis tubing (molecular weight cutoff, 3 KDa). After 48 h, the product was dried in vacuum.

Synthesis of FA-Conjugated GPPS. FA (200 mg) was added into 30 mL of anhydrous DMF and stirred in the dark. Then, the FA solution was mixed with 100 mg of EDC·HCl and 50 mg of DMAP and stirred for 5 h. 1.5 g of GPPS was added to the mixture and the reaction was carried out in the dark for 24 h. The product, GPPS−FA was dialyzed against deionized water using a dialysis tubing (molecular weight cutoff of 3 kDa) for 48 h and freeze-dried.

Synthesis of Au NCs-PLA-GPPS-FA. Au NCs-PLA-GPPS-FA copolymer was synthesized by reacting the carboxyl groups of Au NCs-Au-PLA-COOH with the hydroxyl group of GPPS-FA in the presence of EDC.HCl and DMAP as the catalysts. Au NCs-PLA-COOH (200 mg) was suspended in 20 mL of anhydrous DMF, EDC·HCl (20 mg), and DMAP (10 mg) were added and stirred at room temperature for 5 h. Then, 600 mg of GPPS−FA in 30 mL of anhydrous DMF was added dropwise into the reaction mixture. The reaction was carried out at room temperature for 24 h under stirring. Finally, the products were then dialyzed against deionized water for 48 h (molecular weight cutoff of 3 KDa) and freeze-dried. The products were denoted as Au NCs-PLA-GPPS-FA-1 copolymers and Au NCs-PLA-GPPS-FA-2 copolymers.

The routes for synthesis of core−shell structured multifunctional nanocarriers (Au NCs-PLA-GPPS-FA) were showed in Figure 1.

Characterization. Absorbance spectra and measurements were carried out using a Puxi UV-1810 visible spectrophotometer (Beijing, China). ^{1}H NMR spectrum of the samples was recorded on a Bruker AVANCE 600 MHz spectrometer (Rheinstetten, Germany) using tetramethylsilane as an internal standard and $CDCl_3$ and DMSO (d_6) as the solvents at 25 °C. The IR spectra were recorded on a Nicolet 20 NEXUS 670 FT-IR spectrophotometer (Ramsey, MA, USA) using KBr pellets. Fluorescence spectra of Au NCs and the nanocarriers were recorded on a RF-5301PC fluorescence spectrometer (Shimadzu, Japan) at room temperature. The sizes of Au NCs and the nanocarriers were determined by a BI-200SM DLS (Brookhaven, USA) with angle detection at 90°. The morphology of the samples was recorded by a Tecnai-G2-F30 TEM (FEI, USA).

Drug Loading and Release In vitro. CPT was loaded into the nanocarriers as follows: the nanocarriers (30 mg) were added to 30 mL of DMF solutions including CPT (1 mg/mL) and stirred for 24 h at room temperature until CPT concentration in the solution stabilized. Then the suspension was centrifuged for 10 min at 10000 r/min. To remove free CPT, the nanocarriers were further rinsed by three times using DMF. All the upper clear solutions were collected, and the concentration of free CPT was determined by UV−visible spectrometry at 366 nm. The loading amount was calculated from the

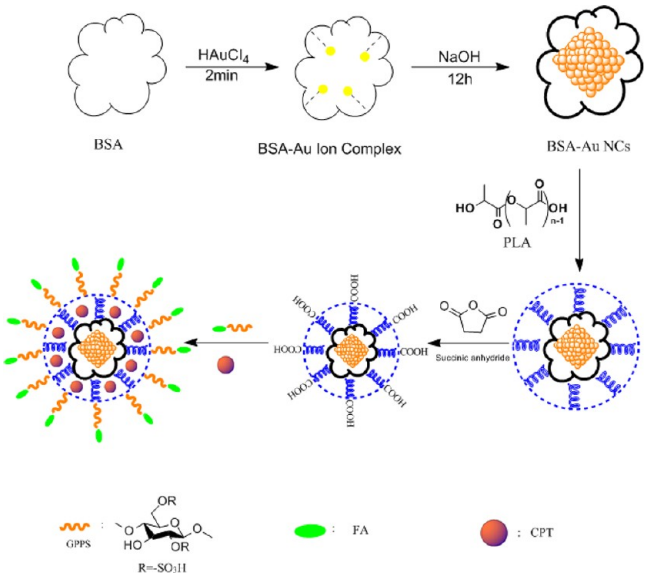

Figure 1. Schematic illustration of the Au NCs-PLA-GPPS-FA copolymers.

decrease in CPT concentration. All the experiments were carried out in triplicate.

The in vitro release behavior was evaluated by the dialysis method. The release studies were performed at 37 °C in acetate buffer (pH 5.3), phosphate buffer (PBS, pH 7.4) and borate buffer (BBS, pH 9.6) solutions. First, 30 mg of the CPT-loaded Au NCs-PLA-GPPS-FA-1 copolymers and Au NCs-PLA-GPPS-FA-2 copolymers was dispersed in 5 mL of medium and placed in a dialysis bag (molecular weight cutoff of 3 kDa), respectively. The dialysis bag was then immersed in 45 mL of the release medium and kept in gentle shaker maintaining a constant temperature. Samples (1 mL) were periodically removed and replaced by the same volume of fresh medium. The amount of released CPT was analyzed with a spectrophotometer at 366 nm. The drug release studies were performed in triplicate for each of the samples.

In vitro Cytotoxicity. The cytotoxicity of the free and the CPT-loaded nanocarriers was assessed by using the MTT assay. For these studies, uterine cervix carcinoma cell line (Hela) and the human lung adenocarcinoma cell line (A549) were provided by the Biology Preservation Center in Shanghai Institute of Materia Medica and maintained with RPMI 1640 medium containing 10% fetal bovine serum (FBS), and 100 U/mL penicillin and 100 μg/mL streptomycin at 37 °C in a humidified atmosphere with 5% CO_2. The cells (1×10^4 cells/well) were seeded into 96-well plates and incubated for 24 h, respectively. Then the blank nanocarriers, the CPT-loaded nanocarriers and the free CPT with different concentration were added. After incubation for 48 h at 37 °C, the culture medium was removed and 20 μL of MTT reagent (diluted in culture medium, 0.5 mg/mL) was added. Following incubation for 4 h, the MTT/medium was removed carefully and DMSO (150 μL) was added to each well for dissolving the formazan crystals. Absorbance of the colored solution was measured at 570 nm using a microplate reader (Bio-Rad, iMark). All experiments were performed in triplicate.

Confocal Microscopy. The confocal scanning microscopy (LEICA TCS SP2) was used for live Hela cell imaging. The Hela cells (1×10^4 cells/well) were seeded on a 6-well plate 37 °C overnight. After that, the CPT-loaded Au NCs-PLA-GPPS-FA-1 copolymers and the CPT-loaded Au NCs-PLA-GPPS-FA-2 copolymers (40 μg/mL) were added, respectively. After a further 10 min and 1.5 h incubation, the cells were washed by PBS three times to remove the nanocarriers adsorbed on the outer surface of cell membrane. Finally, the cells were imaged by the laser scanning confocal microscope under excitation wavelength of 496 nm.

RESULTS AND DISCUSSION

Synthesis and Structural Characterization of Au NCs-PLA-GPPS-FA Copolymer. The reaction scheme of Au NCs-PLA-GPPS-FA copolymers was shown in Figure 1. First, BSA functionalized fluorescent Au NCs could be obtained through a green biomineralization process and applied for drug delivery. The ^{1}H NMR spectrum of Au NCs was shown in Figure 2A. The peaks at about 4.69 ppm (a) and 3.45 ppm (b) were ascribed to the protons of methine and methylene groups in the BSA chains, respectively. The Au NCs as core was designed to emit fluorescent light for optical sensing and cellular imaging.

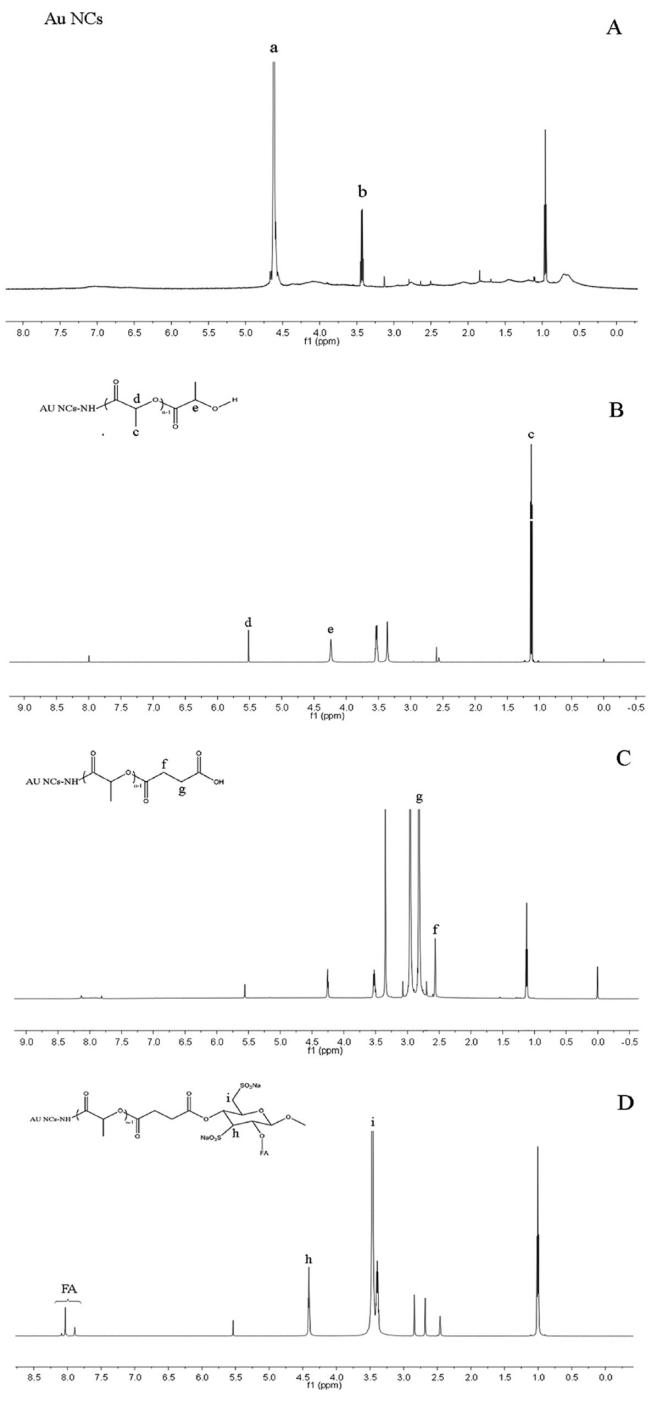

Figure 2. ^{1}H NMR spectra of (A) Au NCs; (B) Au NCs-PLA-1; (C) Au NCs-PLA-COOH; (D) Au NCs-PLA-GPPS-FA-1.

dx.doi.org/10.1021/am301223n | ACS Appl. Mater. Interfaces 2012, 4, 5766−5774

In the second step, the shell of the nanocarriers was synthesized by first coating a hydrophobic PLA layer onto Au NCs core and then using this hydrophobic layer as a seed for the subsequent formation of the hydrophilic GPPS-FA layer. Au NCs-PLA-1 was synthesized by reacting the surface amine groups of Au NCs with some of the terminal carboxyl group of PLA by the amide linkage. The ^{1}H NMR spectrum of Au NCs-PLA-1 was shown in Figure 2B. The peaks at about (c) 1.20 ppm and (d) 5.52 ppm were ascribed to the protons of methyl and methine groups in the PLA main chains, respectively. Moreover, the signal at (e) 4.24 ppm that corresponds with the terminal methine protons of PLA could also be identified. These results confirmed the formation of Au NCs−PLA-1. In the third step, the hydroxyl end groups of Au NCs−PLA-1 were converted into the carboxyl end groups by reacting Au NCs−PLA-1 with succinic anhydride. The ^{1}H NMR spectrum of Au NCs−PLA−COOH (Figure 2C) exhibited two new peaks at 2.78 ppm and 2.96 ppm (methylene groups of succinic anhydride, f and g), which confirmed the synthesis of Au NCs−PLA−COOH. Finally, Au NCs-PLA-GPPS-FA-1 copolymers were obtained by reacting the terminal carboxyl group of Au NCs-PLA-COOH with some of the hydroxyl groups of GPPS-FA by ester forming reaction. In the ^{1}H NMR spectrum of Au NCs-PLA-GPPS-FA-1 (Figure 2D), in addition to the peaks from GPPS-FA blocks, the peaks at 4.42 ppm (h) and 3.50 ppm (i) were observed because of the methine protons and methylene protons of GPPS, respectively. The presence of FA molecule in the product was confirmed by the appearance of weak signals at 7.5−8.5 ppm, which corresponded to the aromatic protons of FA.

The primary structures of Au NCs-PLA-GPPS-FA copolymers were identified by comparing their FT-IR absorption bands to those of Au NCs, PLA, and GPPS-FA (Figure 3). The

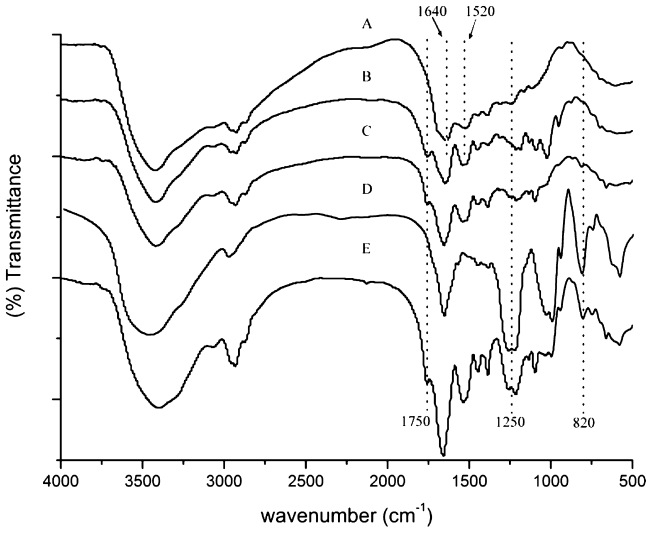

Figure 3. FT-IR spectra of (A) Au NCs; (B) Au NCs-PLA-1; (C) Au NCs-PLA-COOH; (D) GPPS-FA; (E) Au NCs-PLA-GPPS-FA-1.

characteristic absorption of BSA functionalized Au NCs appeared at 1640 cm^{-1} and 1520 cm^{-1} (Figure 3A), corresponding to the C═O bond stretching vibration and the -NH vibration of a −CONH$_2$ group. In Figure 3B, two absorption peaks at 1640 and 1520 cm^{-1} was much stronger, assigned to the new bond of −CONH$_2$ group on the Au NCs-PLA-1. A new strong absorption peaks appeared at 1750 cm^{-1}, assigned to the stretching vibrations of C═O groups of PLA on the Au NCs-PLA-1, which indicated that PLA was modified successfully on the surface of Au NCs. Compared with Figure 3B, the characteristic band of the terminal carboxyl group of Au NCs-PLA-COOH was buried in the strong C═O groups of PLA (Figure 3C). In Figure 3D, two strong absorption peaks appeared at 1250 and 820 cm^{-1}, assigned to the S═O asymmetric stretching and C−O−S symmetric vibrations of GPPS, respectively. Furthermore, two weak absorption peaks at 1600 and 1500 cm^{-1} was due to the characteristic absorption of the benzene ring of FA. Finally, the FT-IR spectrum of Au NCs-PLA-GPPS-FA-1 copolymers showed the characteristic absorption bands of both PLA and GPPS-FA (Figure 3E), which confirmed successful synthesis of Au NCs-PLA-GPPS-FA copolymers.

Properties of Au NCs-PLA-GPPS-FA Copolymers. The photoluminescence (PL) spectra of Au NCs, Au NCs-PLA-GPPS-FA-1 copolymers, and Au NCs-PLA-GPPS-FA-2 copolymers aqueous solutions was shown at the same concentration (1 mg/mL) in Figure 4A, respectively. The fluorescent Au NCs showed emission peaks at 620 nm when excited at 480 nm. Highly fluorescent Au NCs with red emissions was synthesized successfully. At the same time, two kinds of the nanocarriers displayed a symmetric PL emission at 620 nm when excited at 480 nm, which was similar to the PL spectra of Au NCs. Au NCs were coated with an inner PLA layer and a subsequent external GPPS-FA layer, but the change of the PL intensity of the nanocarriers was not prominent. The slight variation in the PL intensity was possibly due to the change in the refractive index of the shell of the nanocarriers and any quenching effects by the interlayers interaction on the nanocarriers when the GPPS-FA layer swelled and shrunk.[26] Figure 4B exhibited strong red emission from Au NCs, Au NCs-PLA-GPPS-FA-1 copolymers and Au NCs-PLA-GPPS-FA-2 copolymers aqueous solutions under UV light (360 nm), and the photograph of aqueous solutions was also presented as a blank comparison.

The size and stability of drug carriers are important properties that influence their performance in vivo. On the basis of physiological parameters such as hepatic filtration, tissue extravasation, tissue diffusion, and kidney excretion, it is clear that particle size is a key factor in the biodistribution of long-circulating nanoparticles and achieving therapeutic efficacy.[27,28] The nanoparticle carriers in the size range of 10−100 nm have actual advantages to improve the blood circulation time and enhance the extravasation rate into permeable tissues such as tumors.[27−29] The size distribution of the AuNCs and copolymers was determined by DLS. Figure 5A showed the size distribution of Au NCs, and Au NCs had a narrow size distribution ranging from 1.0 to 1.7 nm with an average particle size diameter of 1.28 nm. However, the size distribution of Au NCs-PLA-GPPS-FA-1 copolymers and Au NCs-PLA-GPPS-FA-2 copolymers was relatively broad, ranging from 20 to 45 nm and from 30 to 80 nm, respectively. The average size was 32 and 47 nm, respectively (Figure 5B and C). The increased size and size distribution of the nanocarriers might be due to the existence of a fairly thick PLA and GPPS-FA on the surface of Au NCs.

The size and morphology of Au NCs, Au NCs-PLA-GPPS-FA-1 copolymers, and Au NCs-PLA-GPPS-FA-2 copolymers were further illustrated by TEM in Figure 6. Au NCs showed spherical particles with high dispersion and good crystalline nature (Figure 6A, B). In Figure 6C and E, Au NCs-PLA-GPPS-FA-1 copolymers and Au NCs-PLA-GPPS-FA-2 copoly-

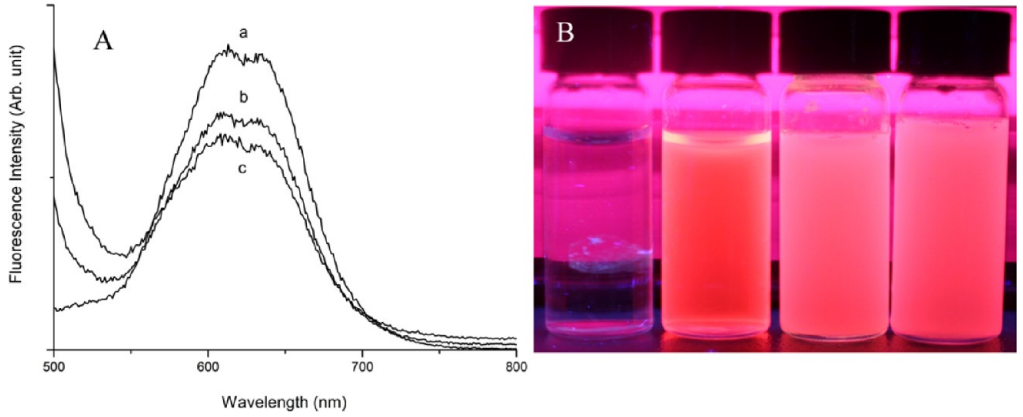

Figure 4. (A) Typical PL spectra of (a) Au NCs, (b) Au NCs-PLA-GPPS-FA-1 copolymers, and (c) Au NCs-PLA-GPPS-FA-2 copolymers were obtained with the excitation wavelength at 480 nm. (B) Photograph of the samples from left to right was aqueous solutions, Au NCs, Au NCs-PLA-GPPS-FA-1 copolymers, and Au NCs-PLA-GPPS-FA-2 copolymers under UV light (1 mg/mL).

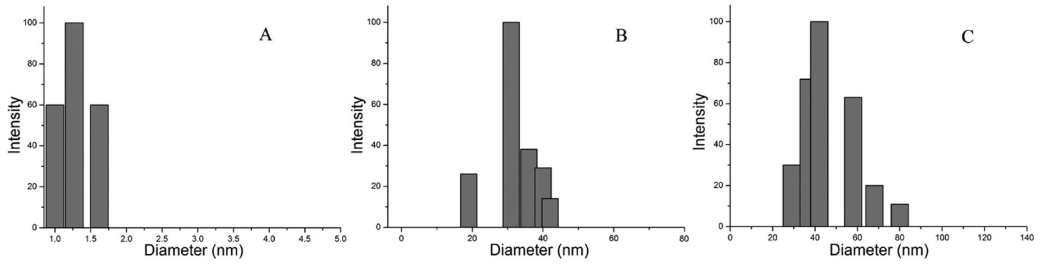

Figure 5. Size distribution of (A) Au NCs; (B) Au NCs-PLA-GPPS-FA-1 copolymers; (C) Au NCs-PLA-GPPS-FA-2 copolymers.

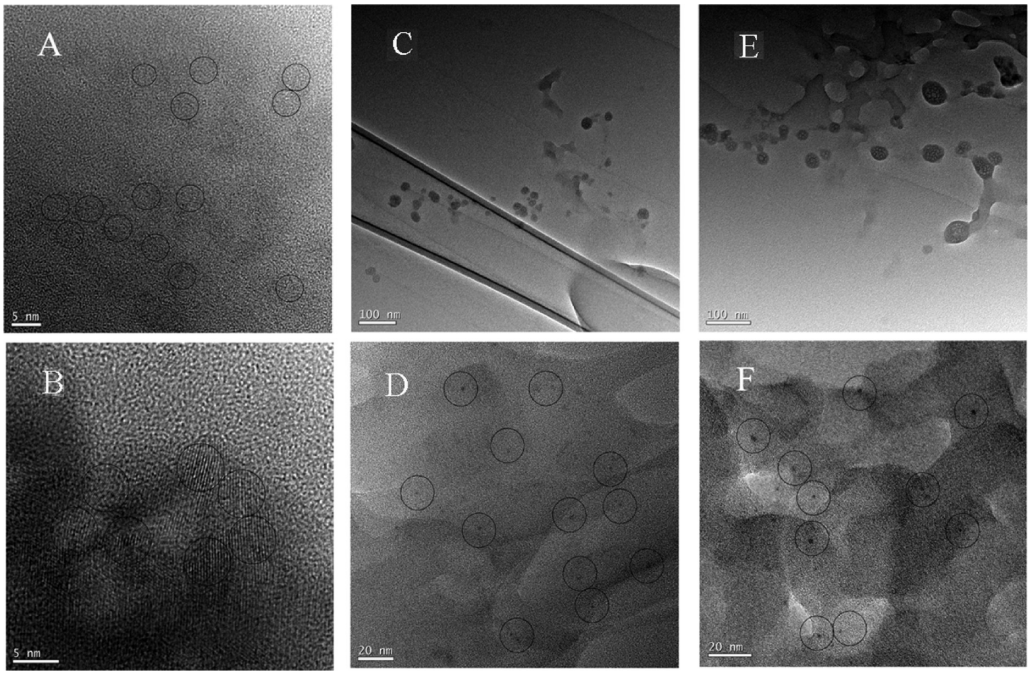

Figure 6. TEM images of (A, B) Au NCs; (C, D) Au NCs-PLA-GPPS-FA-1 copolymers; (E, F) Au NCs-PLA-GPPS-FA-2 copolymers.

mers appeared spherical particles, and the size distribution was in the range of 15−35 nm and 20−55 nm, which was an appropriate size for effective endocytosis. Furthermore, TEM morphology data also clarified the existence of Au NCs within two kinds of copolymers in panels D and F in Figure 6, respectively. In addition, two kinds of the nanocarriers was little agglomeration due to amphiphilic PLA-GPPS-FA copolymer on the Au NCs core preventing the nanocarriers from aggregation. The diameter of two kinds of the nanocarriers was smaller than the value obtained from the DLS measurement. The larger diameter from the DLS experiment relative to TEM was most likely due to the existence of a swollen GPPS-FA around the core. The size range of two kinds of the nanocarriers determined by DLS and TEM was desirable for

dx.doi.org/10.1021/am301223n | ACS Appl. Mater. Interfaces 2012, 4, 5766−5774

drug carriers to extend their blood circulation time, and the FA-receptor-mediated endocytosis process that leaded to the preferred accumulation of drug-conjugated micelles within tumors.[30]

Drug Loading and Release. To assess the feasibility of the nanocarriers as the anticancer drug delivery carriers, we studied drug loading yield and release behavior in vitro using Au NCs-PLA-GPPS-FA-1 copolymers and Au NCs-PLA-GPPS-FA-2 copolymers under an acidic environment (pH 5.3), a simulated physiological condition (pH 7.4) and an alkaline environment (pH 9.6). Typically, CPT was loaded into the nanocarriers in a DMF solution. The loading efficiency of CPT was 4.7 and 6.3 wt % for Au NCs-PLA-GPPS-FA-1 copolymers and Au NCs-PLA-GPPS-FA-2 copolymers, respectively. A blank release experiment of free CPT solution with an equivalent amount of drug was also carried out at pH 7.4 (Figure 7A). This study

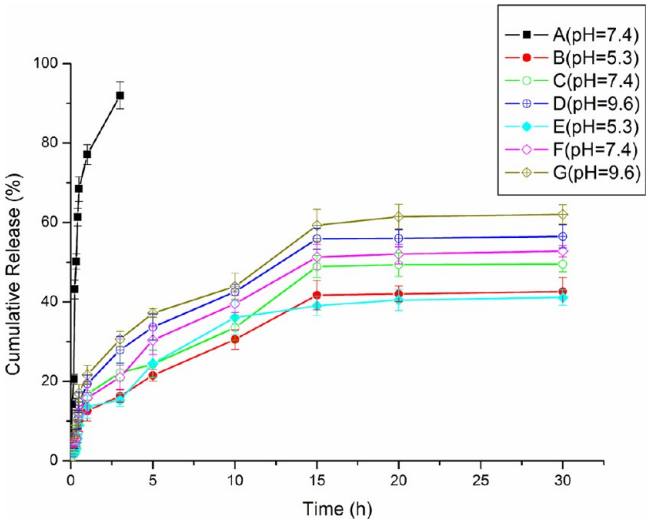

Figure 7. In the blank release (A), 5 mL of free CPT solution was released to 45 mL PBS solution of pH 7.4 at 37 °C. Release profiles of CPT from the CPT-loaded Au NCs-PLA-GPPS-FA-1 (B–D) and Au NCs-PLA-GPPS-FA-2 copolymers (E–G) were obtained at acidic conditions (pH 5.3), neutral conditions (pH 7.4), and alkaline conditions (pH 9.6) at 37 °C.

suggested that free CPT presented a rapid release (77% of the initial loading amount) in 1 h, which indicated that the dialysis membrane played negligible role in the release of CPT. Both CPT loaded Au NCs-PLA-GPPS-FA-1 copolymers and Au NCs-PLA-GPPS-FA-2 copolymers presented a relatively rapid release in the first stage (up to 1 h) followed by a sustained release period (up to 15 h), and then reached a plateau at pH 5.3, 7.4, and 9.6. Compared with the blank experiment, the much slower release rate of CPT from the nanocarriers than that from the free CPT solution demonstrated a sustained release of CPT from the nanocarriers. The initial burst release of CPT from the nanocarriers might be simple adsorption or weak interaction between CPT molecules located within the hydrophilic shell and the hydrophilic shell. The sustained release of the drug from NCs could be attributed to the hydrophobic–hydrophobic interactions between the drug molecules and the hydrophobic polymer (PLA).

Moreover, the change in pH of the releasing medium could trigger the drug releasing rate in Figure 7. The amount and rate of CPT release from two kinds of the nanocarriers at pH 9.6 were much greater when compared to that at both pH 5.3 and 7.4. At pH 5.3, the initial burst release of CPT for Au NCs-PLA-GPPS-FA-1 copolymers and Au NCs-PLA-GPPS-FA-2 copolymers was 13% and 14% of the initial loading amount, respectively. The sustained release of CPT reached a plateau in 15 h, and the release amount was 41% and 39%, respectively. At pH 9.6, the CPT release rate of Au NCs-PLA-GPPS-FA-1 copolymers and Au NCs-PLA-GPPS-FA-2 copolymers was faster (19 and 22% of the initial loading amount) in the first 1 h and the sustained release (55 and 59% of the initial loading amount) reached a plateau in 15 h. The PLA segments swelled at high pH value, which gave rise to the mobility of CPT molecules. Subsequently, CPT leaked from the nanocarriers easily. As a result, rapid drug release behavior could be found when the pH value is higher.

Comparing with the CPT release profiles in Figure 7, we found that the release behaviors of CPT were very similar in two kinds of the nanocarriers, indicated that the release obeyed a diffusion-controlled mechanism; however, the diffusion rates at each stage of the drug release differed considerably, suggesting that two different processes might be taking place. In the initial burst stage, drug release occurred faster. During this time, the drug presented on the surface of hydrophilic outer shell might have good access to the surrounding aqueous environment through the surface of the nanocarriers. However, in the sustained release period, the drug loading could be entrapped in the dense solid regions of the hydrophobic inner

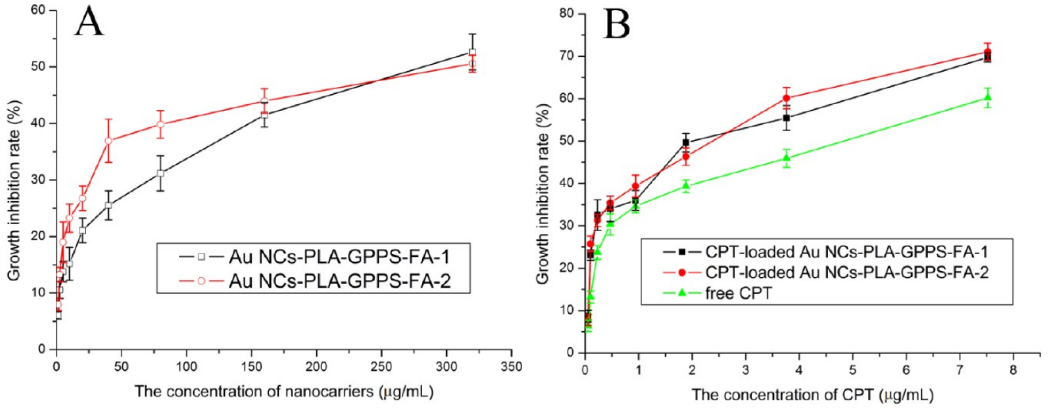

Figure 8. (A) In vitro cytotoxicity of the blank Au NCs-PLA-GPPS-FA-1 and Au NCs-PLA-GPPS-FA-2 copolymers against Hela cells, respectively. (B) Cytotoxicity of free CPT, the CPT-loaded Au NCs-PLA-GPPS-FA-1, and Au NCs-PLA-GPPS-FA-2 copolymers against Hela cells.

dx.doi.org/10.1021/am301223n | ACS Appl. Mater. Interfaces 2012, 4, 5766–5774

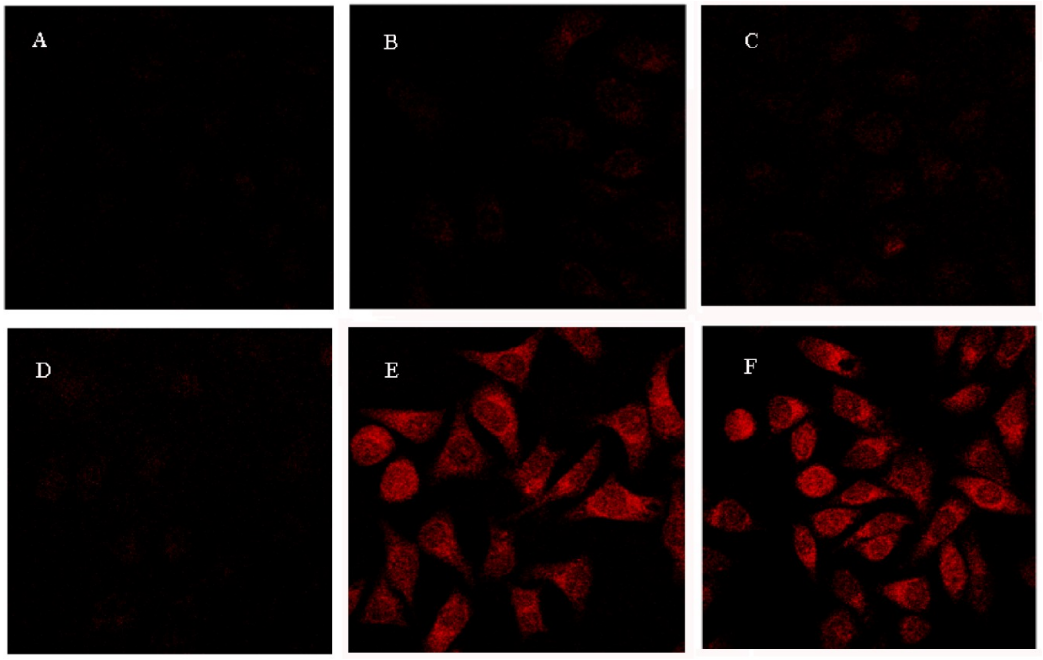

Figure 9. Scanning confocal images of Hela cells incubated with (A, D) the control experiment, (B, E) the CPT-loaded Au NCs-PLA-GPPS-FA-1 copolymers, (C, F) the CPT-loaded Au NCs-PLA-GPPS-FA-2 copolymers at 37 °C for 10 min and 1.5 h, respectively.

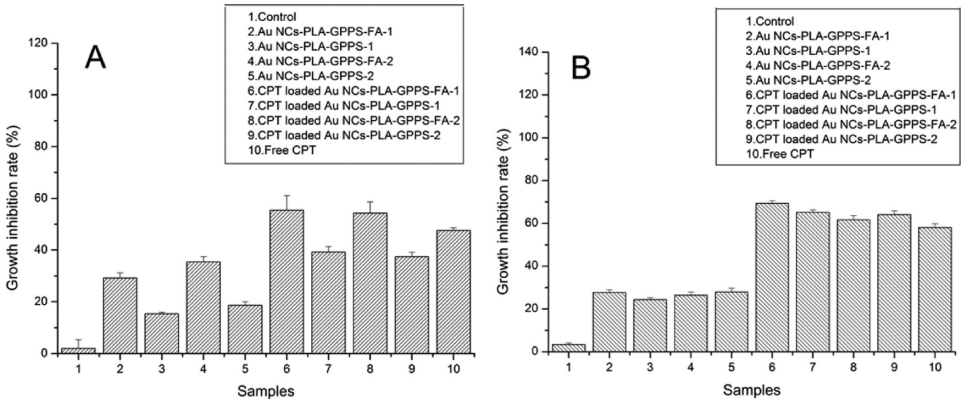

Figure 10. Cytotoxicity of free CPT, Au NCs-PLA-GPPS, Au NCs-PLA-GPPS-FA, CPT-loaded Au NCs-PLA-GPPS, and Au NCs-PLA-GPPS-FA copolymers against (A) Hela cells and (B) A549 cells.

shell where polymer entanglement serves as a much greater impediment to drug transport.

In vitro Cytotoxicity. The cytotoxicity effects of the blank nanocarriers and the CPT loaded nanocarriers against Hela cells were evaluated in vitro. HeLa cells were FA receptor overexpressing cells. The potential cytotoxicity with the corresponding CPT concentrations was also studied. As shown in Figure 8A, the blank nanocarriers had a mild cytotoxicity to Hela cells with the increase of nanocarriers concentration for Au NCs-PLA-GPPS-FA-1 copolymers and Au NCs-PLA-GPPS-FA-2 copolymers. Furthermore, the inhibition rates of the CPT-loaded nanocarriers in Figure 8B were higher than that of the free CPT solutions since the CPT amounts were at the same levels. This was likely because the nanocarriers had certain antitumor activities due to GPPS on the surface of the nanocarriers, which would be more effective to kill tumor cells by the cooperation of carriers and drugs. Thus, the slightly higher cytotoxicity of the CPT-loaded nanocarriers than the free CPT solutions was understandable. These results indicated that the CPT-loaded nanocarriers provided high anticancer activity.

Tumour Cell Imaging. Figure 9 showed fluorescent images taken at two time points 10 min and 1.5 h incubation. In the control experiment, Hela cells without the nanocarriers were used as a negative control and showed only much weaker autofluorescence of the cells (Figure 9A, D). In the first 10 min of incubation, only weaker fluorescence was observed (Figure 9B, C), indicating very few nanocarriers are internalized into the cells by short time contact with the cells. At 1.5 h, plenty of nanocarriers were uptaken by the cells and exhibited bright and stable red fluorescence in the cytoplasm of the cells (Figure 9E, F). For the CPT-loaded Au NCs-PLA-GPPS-FA-1 copolymers and the CPT-loaded Au NCs-PLA-GPPS-FA-2 copolymers, the cellular uptake was mainly based on the small size and endocytosis mechanism that might result in a greater amount of the nanocarriers internalized inside tumor cells. These results revealed that the nanocarriers designed in this work could act as intracellular drug delivery systems and thus be tracked or monitored at the cellular level for advance therapy.

dx.doi.org/10.1021/am301223n | ACS Appl. Mater. Interfaces 2012, 4, 5766−5774

In vitro FA Targeting. To directly define a role for FA targeting, we studied free CPT (4 μg/mL), and two kinds of blank or CPT loaded nanocarriers (CPT concentration: 4 μg/mL) against Hela cells (folate receptor overexpressing cell line) and A549 cells (folate receptor deficient cell line). As shown in Figure 10 A, compared with blank or CPT loaded Au NCs-PLA-GPPS-1 NCs and Au NCs-PLA-GPPS-2 NCs, blank or CPT-loaded Au NCs-PLA-GPPS-FA-1 NCs and Au NCs-PLA-GPPS-FA-2 NCs exhibited higher inhibition ratio against Hela cells, respectively. The results clearly showed that the cytotoxicity of two kinds of nanocarriers with FA against Hela cells was greater than two kinds of nanocarriers without FA. The increased cytotoxicity of two kinds of nanocarriers with FA against Hela cells was most likely due to the folate-receptor-mediated endocytic uptake of Au NCs-PLA-GPPS-FA-1 copolymers and Au NCs-PLA-GPPS-FA-2 copolymers, which led to greater cellular uptake of CPT and thus greater cytotoxicity. However, there was no significant difference in inhibition ratio of A549 cells when cultured in the presence of Au NCs-PLA-GPPS NCs and Au NCs-PLA-GPPS-FA NCs (Figure 10B). This observation showed that the FA molecule present on the surface of nanocarriers did not have any effect on the A549 cells cellular uptake. The observed cytotoxicity may be due to the cellular uptake of CPT in the nanocarriers which could diffuse into the cells.

Compared with FA-free CPT-loaded Au NCs-PLA-GPPS-1 copolymers and CPT-loaded Au NCs-PLA-GPPS-2 copolymers, the extent of cellular uptake of the CPT-loaded Au NCs-PLA-GPPS-FA-1 copolymers and the CPT-loaded Au NCs-PLA-GPPS-FA-2 copolymers was evaluated to understand the effect of FA on cellular uptake. As shown in A and B in Figure 11, weaker fluorescence was observed in the cytoplasm. In contrast, strong red fluorescence was found primarily in the cytoplasm of Hela cells (Figure 11C, D). These results further indicated that the cellular uptake of the CPT-loaded Au NCs-PLA-GPPS-FA-1 copolymers and the CPT-loaded Au NCs-PLA-GPPS-FA-2 copolymers was mainly based on a folate-receptor-mediated endocytosis mechanism that might resulted in a greater amount of nanocarriers internalized inside tumor cells.

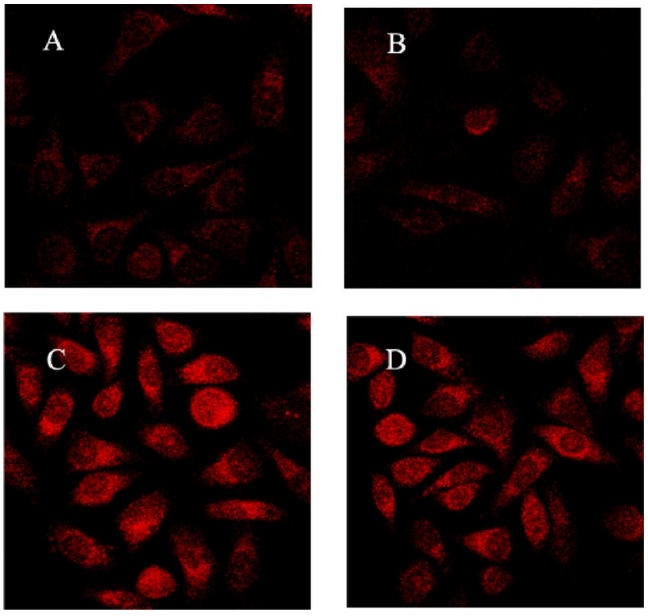

Figure 11. Scanning confocal images of Hela cells incubated with (A, C) the CPT-loaded Au NCs-PLA-GPPS-1 and CPT-loaded Au NCs-PLA-GPPS-FA-1 copolymers, respectively, (B, D) the CPT-loaded Au NCs-PLA-GPPS-2 and CPT-loaded Au NCs-PLA-GPPS-FA-2 copolymers at 37 °C for 1.5 h, respectively.

CONCLUSION

We prepared two kinds of FA-conjugated amphiphilic Au NCs-PLA-GPPS-FA copolymers as the tumor-targeted drug delivery carriers. ^{1}H NMR spectra and FT-IR spectra indicated that two kinds of the nanocarriers had been synthesized successfully. And they displayed strong red emission at 620 nm when excited at 480 nm. The size distribution of Au NCs-PLA-GPPS-FA-1 copolymers and Au NCs-PLA-GPPS-FA-2 copolymers was relatively broad, ranging from 20 to 45 nm and from 30 to 80 nm by DLS, and was in the range of 15−35 nm and 20−55 nm by TEM, respectively.

The release in vitro indicated that two kinds of the nanocarriers could be a very promising vehicle for the administration of controlled release of hydrophobic anticancer drugs. The strong hydrophobic interactions of the hydrophobic PLA with the drug molecules could be a main reason for the slow and steady release of the CPT from the nanocarriers. The release rate of CPT from the nanocarriers was significantly accelerated by increasing pH. The nanocarriers provided high anticancer activity and showed the specificity to target some cancer cells due to the enhanced cell uptake mediated by FA moiety. Furthermore, the nanocarriers could be tracked at the cellular level for advance therapy. These results indicated that the Au NCs-PLA-GPPS-FA copolymers could be not only an excellent tumor-targeted drug delivery nanocarrier but also had an assistant role in the treatment of cancer.

AUTHOR INFORMATION

Corresponding Author

*Tel.: +86 931 8912510. Fax: +86 931 8912582. E-mail: zhanghx@lzu.edu.cn; zhaochy07@lzu.edu.cn.

Notes

The authors declare no competing financial interest.

ACKNOWLEDGMENTS

This work was supported by the Fundamental Research Funds for the Central Universities (no. lzujbky-2012-k09) and the National Natural Science Foundation of China (NSFC) Fund (21105039). The authors thank the Key Laboratory of Chemistry of Northwestern Plant Resources, Lanzhou Institute of Chemical Physics, Chinese Academy of Sciences for its fund supporting (CNPR-2012kfkt-10).

REFERENCES

(1) Negishi, Y.; Takasugi, Y.; Sato, S.; Yao, H.; Kimura, K.; Tsukuda, T. *J. Am. Chem. Soc.* **2004**, *126*, 6518.
(2) Wu, Z.; Jin, R. *Nano Lett.* **2010**, *10*, 2568.
(3) Huang, C. C.; Chen, C. T.; Shiang, Y. C.; Lin, Z. H.; Chang, H. T. *Anal. Chem.* **2009**, *81*, 875.
(4) Guo, W.; Yuan, J.; Dong, Q.; Wang, E. *J. Am. Chem. Soc.* **2009**, *132*, 932.
(5) Hong, R.; Han, G.; Fernandez, J. M.; Kim, B. J.; Forbes, N. S.; Rotello, V. M. *J. Am. Chem. Soc.* **2006**, *128*, 1078.
(6) Prabaharan, M.; Grailer, J. J.; Pilla, S.; Steeber, D. A.; Gong, S. Q. *Biomaterials* **2009**, *30*, 6065.
(7) Zhu, M.; Lanni, E.; Garg, N.; Bier, M. E.; Jin, R. *J. Am. Chem. Soc.* **2008**, *130*, 1138.

(8) Lin, C. A. J.; Yang, T. Y.; Lee, C. H.; Huang, S. H.; Sperling, R. A.; Zanella, M.; Li, J. K.; Shen, J. L.; Wang, H. H.; Yeh, H. I.; Parak, W. J.; Chang, W. H. *ACS Nano* **2009**, *3*, 395.
(9) Zhu, M.; Aikens, C. M.; Hollander, F. J.; Schatz, G. C.; Jin, R. J. *J. Am. Chem. Soc.* **2008**, *130*, 5883.
(10) Negishi, Y.; Nobusada, K.; Tsukuda, T. *J. Am. Chem. Soc.* **2005**, *127*, 5261.
(11) Xie, J. P.; Zheng, Y. G.; Ying, J. Y. *J. Am. Chem. Soc.* **2009**, *131*, 888.
(12) Liu, Y.; Ai, K.; Cheng, X.; Huo, L.; Lu, L. *Adv. Funct. Mater.* **2010**, *20*, 951.
(13) Wen, F.; Dong, Y. H.; Feng, L.; Wang, S.; Zhang, S. C.; Zhang, X. R. *Anal. Chem.* **2011**, *83*, 1193.
(14) Siegwart, D. J.; Srinivasan, A.; Bencherif, S. A.; Karunanidhi, A.; Vaidya, S.; Jin, R. C.; Hollinger, J. O.; Matyjaszewski, K. *Biomacromolecules* **2009**, *10*, 2300.
(15) Kopac, T.; Bozgeyik, K.; Yener, J. *Colloids Surf., A* **2008**, *322*, 19−28.
(16) Rujjanawate, C.; Kanjanapothi, D.; Amornlerdpison, D. *Phytomedicine* **2004**, *11*, 431.
(17) Qian, X. H.; Wang, Y. X.; Tang, X. L. *J. China Pharm. Univ.* **1998**, *30*, 51.
(18) Birgitte, L. C.; Per, M.; Zhao, Y. J. *Ethnopharmacol.* **1995**, *46*, 125.
(19) Chen, T.; Li, B.; Li, Y. Y.; Zhao, C. D.; Shen, J. M.; Zhang, H. X. *Carbohyd. Polym.* **2011**, *83*, 554.
(20) Allen, T. M.; Cullis, P. R. *Science* **2004**, *303*, 1818.
(21) Lee, C. C.; MacKay, J. A.; Frechet, J. M. J.; Szoka, F. C. *Nat. Biotechnol.* **2005**, *23*, 1517.
(22) Torchilin, V. P. *Nat. Rev. Drug Discov.* **2005**, *4*, 145.
(23) Peer, D.; Karp, J. M.; Hong, S.; Farokhzad, O. C.; Margalit, R.; Langer, R. *Nat. Biotechnol.* **2007**, *2*, 751.
(24) Leamon, C. P.; Reddy, J. A. *Adv. Drug Deliver. Rev.* **2004**, *56*, 1127.
(25) Chen, S.; Zhang, X. Z.; Cheng, S. X.; Zhuo, R. X.; Gu, Z. W. *Biomacromolecules* **2008**, *9*, 2578.
(26) Wu, W.; Zhou, T.; Berliner, A.; Banerjee, P.; Zhou, S. *Chem. Mater.* **2010**, *22*, 1966.
(27) Alexis, F.; Pridgen, E.; Molnar, L. K.; Farokhzad, O. C. *Mol. Pharmacol.* **2008**, *5*, 505.
(28) Schmalenberg, K. E.; Frauchiger, L.; Nikkhouy-Albers, L.; Uhrich, K. E. *Biomacromolecules* **2001**, *2*, 851.
(29) Lukyanov, A.; Gao, Z.; Mazzola, L.; Torchilin, V. P. *Pharm. Res.* **2002**, *19*, 1424.
(30) Yuan, F.; Dellian, M.; Fukumura, D.; Leunig, M.; Berk, D. A.; Torchilin, V. P. *Cancer Res.* **1995**, *55*, 3752.